YlmD and YlmE are required for correct sporulation-specific cell division in *Streptomyces coelicolor* A3(2)

Le Zhang[1], Joost Willemse[1], Paul A. Hoskisson[2] and Gilles P. van Wezel[1, *]

[1] *Molecular Biotechnology, Institute of Biology, Leiden University, Sylviusweg 72, 2333 BE, The Netherlands*

[2] *Strathclyde Institute of Pharmacy and Biomedical Science, University of Strathclyde, 161 Cathedral Street, Glasgow, G4 0RE, United Kingdom*

* Author for correspondence. Tel: +31 71 5274310; email: g.wezel@biology.leidenuniv.nl.

ABSTRACT

Cell division during the reproductive phase of the *Streptomyces* life-cycle requires tight coordination between synchronous formation of multiple septa and DNA segregation. One remarkable difference with most other bacterial systems is that cell division in *Streptomyces* is positively controlled by the recruitment of FtsZ by SsgB. Here we show that the genes *ylmD* (SCO2081) and *ylmE* (SCO2080), which lie in operon with *ftsZ* in the *dcw* cluster of actinomycetes, are required for correct sporulation-specific cell division in *Streptomyces coelicolor*. Electron and fluorescence microscopy demonstrated that in particular *ylmE* mutants have a highly aberrant phenotype with defective septum synthesis, and produce very few spores with aberrant spore walls. FtsZ-ring formation was disturbed in *ylmD* and *ylmE* mutants. YlmD and YlmE are not part of the divisome, but instead localise diffusely in aerial hyphae, with differential intensity throughout the sporogenic part of the hyphae. Taken together, our work shows that YlmD and YlmE play an important role in (the control of) sporulation-specific cell division, with a more dominant role for YlmE, likely supported by YlmD. This sheds light on the function of the two genes in the direct vicinity of *ftsZ* whose function had sofar remained unresolved.

INTRODUCTION

In unicellular bacteria, cell division divides a mother cell in two identical daughter cells, each containing a single copy of the chromosome. The control of cell division thereby revolves around finding the mid-cell position, and chromosome segregation and septum synthesis are closely coordinated in time and space to avoid DNA damage by the nascent septum . The cell division scaffold is formed by FtsZ, which is a homologue of tubulin (Bi and Lutkenhaus, 1991) and forms a contractile ring (or Z-ring) that mediates the recruitment of the cell division machinery to the division site (reviewed in (Adams and Errington, 2009; Goehring and Beckwith, 2005)). Septum-site selection and Z-ring stabilization are mediated by proteins like FtsA and ZipA (Hale and de Boer, 1997; Pichoff and Lutkenhaus, 2002; RayChaudhuri, 1999), ZapA (Gueiros-Filho and Losick, 2002) and SepF (Hamoen *et al.*, 2006; Ishikawa *et al.*, 2006). Z-ring (dis-)assembly is thereby actively controlled (reviewed in (Romberg and Levin, 2003)).

Streptomycetes are filamentous Gram-positive bacteria that belong to the phylum of Actinobacteria. These bacteria produce over 60% of all known antibiotics and many other bioactive natural products (Barka *et al.*, 2016; Hopwood, 2007). Exponential growth of the vegetative hyphae is achieved by apical growth and branching. At this stage of the life cycle, cell division does not effect physical separation of the cells, but instead long syncytial cells are formed that are separated by crosswalls (Wildermuth and Hopwood, 1970). Hence, streptomycetes are model organisms for the study of multicellularity and bacterial morphogenesis (Claessen *et al.*, 2014; Flärdh and Buttner, 2009). Most divisome components except FtsZ are not required for vegetative division, presumably reflecting the lack of constriction (McCormick, 2009). Spacing between the cross-walls is highly variable, and little is

known of the way septum-site selection is controlled. Recently, using cryo-electron tomography, our lab and others showed that intracellular membrane assemblies or cross-membranes are involved in DNA protection during septum synthesis in young vegetative hyphae, suggesting a novel way of cell-division control (Celler *et al.*, 2016; Yagüe *et al.*, 2016). In addition, these multicellular bacteria have a complex cytoskeleton, which among others plays a role in the organization of the tip growth machinery (Celler *et al.*, 2013; Holmes *et al.*, 2013).

Canonical division resulting in cell fission occurs during sporulation-specific cell division, which requires all components of the divisome (Jakimowicz and van Wezel, 2012; McCormick, 2009). At this stage of the life cycle up to a hundred septa are formed in a short time span, following a highly complex process of coordinated cell division and DNA segregation, and visualized as long ladders of Z-rings (Schwedock *et al.*, 1997). Eventually, chains of unigenomic spores are formed, which have a thick protective spore wall facilitating long-term survival in the environment. While *ftsZ* null mutants fail to produce septa and hence do not sporulate, cell division is not essential for growth of *Streptomyces*, which provides a unique system for the study of this process (McCormick *et al.*, 1994; McCormick and Losick, 1996).

Sporulation-specific cell division is controlled by the SsgA-like proteins (SALPs), which are exclusively found in morphologically complex actinobacteria (Girard *et al.*, 2013; Traag and van Wezel, 2008). The canonical view is that cell division is negatively controlled by the action of the Min system that inhibits division away from midcell, and by nucleoid occlusion (Noc) to avoid septum synthesis near the chromosome to avoid DNA damage, as seen in *B. subtilis* and *E. coli*. In contrast, cell division in streptomycetes is positively controlled by the recruitment of FtsZ to future septum sites by SsgB, in an SsgA-dependent manner (Willemse *et al.*, 2011). As a

consequence, both SsgA and SsgB are required for sporulation (Keijser *et al.*, 2003; van Wezel *et al.*, 2000a). We recently showed that SepG (formerly called YlmG) assists in docking of SsgB to the membrane, and also plays a major role in maintaining the nucleoid shape in the spores (Zhang *et al.*, 2016).

Many of the genes for the components of the divisome and the cell-wall biosynthetic machinery are located in the so-called *dcw* cluster (division and cell-wall synthesis; (Mingorance *et al.*, 2004)). Most of these genes have been studied extensively and their functions have been well characterized. However, little is known of the genes *ylmD* and *ylmE* that lie immediately downstream of, and likely in operon with, *ftsZ* on the genome of streptomycetes and many other bacteria, including firmicutes. In this study we demonstrate that YlmD and YlmE play an important role in cell-wall synthesis during sporulation, whereby in particular *ylmE* null mutants show severe cell division defects, resulting in a near complete block of sporulation in *Streptomyces coelicolor* and *Streptomyces lividans*.

RESULTS & DISCUSSION

Phylogenetic analysis of YlmE (SCO2080) and YlmD (SCO2081)

Many of the genes in the *dcw* gene cluster have been extensively studied and their functions are well established. However, this is not the case for *ylmD* and *ylmE*, which lie immediately downstream of *ftsZ* in many bacteria. In all *Streptomyces* genomes analyzed, *ftsZ* (SCO2082), *ylmD* (SCO2081) and *ylmE* (SCO2080) form an operon, an observation that is supported by high-

resolution transcript mapping (Romero *et al.*, 2014); moreover there is apparent translational fusion between *ftsZ* and *ylmD* (overlapping start and stop codons) and the mere 6 nt spacing between *ylmD* and *ylmE*. This transcriptional coupling to *ftsZ* suggests that these genes may play a prominent role in the cell division process. Transcript levels of *ftsZ* are similar to those of *ylmD* and *ylmE* during vegetative growth on MM agar plates; however, *ftsZ* is transcribed at significantly higher levels during sporulation (Swiatek *et al.*, 2013). YlmD and YlmE are wide-spread in Gram-positive bacteria, and particularly in actinobacteria. SCO2081 and SCO2080 share 32% aa identity with YlmD and YlmE of *B. subtilis*, respectively. Orthologues of these proteins are also found in several genera of Gram-negative bacteria. Phylogenetic analysis of the YlmD and YlmE proteins in actinobacteria shows that while YlmE is widespread, YlmD is often absent in actinobacteria, such as *Stackebrandtia, Catenulispora, Salinispora, Micromonospora, Amycolatopsis* and *Mycobacterium*, several of which are spore-forming actinobacteria (Fig. 1). Remarkably, no examples of *ylmD* being present in the absence of *ylmE* and thus it would appear that loss of YlmD (SCO2081) has occurred on multiple occasions, given that there is wide but patchy distribution of this gene across distinct actinobacteria lineages and the sequences clade tightly within the accepted actinomycete phylogenies. This would suggest that there is potentially overlapping function in these two genes.

Analysis of *ylmD* using the EMBL String engine (Szklarczyk *et al.*, 2011) shows functional linkage in two groups to cell division associated genes (*sepF2,* SCO2085 and ftsZ) along with a group of mainly hypothetical proteins (STRING Data link: http://bit.ly/2gc5kCB). YlmD has a domain that has homology to the multiple-copper polyphenol oxidoreductase laccases, which are oxidoreductases that are widely distributed in both prokaryotes and eukaryotes (Claus,

2003). A similar analysis of YlmE also indicates a functional linkage to cell-wall biosynthesis and cell division (STRING Data link: http://bit.ly/2gbPyHK). YlmE is a YBL036c-like protein which generally contain pyridoxal 5-phosphate dependent enzymes. The structure of YBL036c from *Saccharomyces cerevisiae* was resolved at 2.0 Å resolution (PDB 1CT5;(Eswaramoorthy *et al.*, 2002). The protein has homology to the N-terminal domains of alanine racemases but lacks of the β-sandwich domain which would likely limit the activity of YBL036c as alanine or non-specific amino acid racemase (Percudani and Peracchi, 2003). To test the hypothesis that YlmE may have alanine racemase activity and thus may play a role in determining the amino acid composition of the peptidoglycan, we tested purified YlmE for alanine racemase assays as described previously (Tassoni *et al.*, 2017). YlmE failed to catalyze the conversion of L-alanine to D-alanine *in vitro*, and over-expression of the enzyme also failed to restore a D-Ala auxotrophy to *alr* null mutants (data not shown). These observations coupled with protein structure homology data make it highly unlikely that YlmE functions as an alanine racemase *in vivo*.

ylmD and y_lmE_ are required for proper sporulation

To analyze the role of *ylmD* and *ylmE*, deletion mutants were created in *S. coelicolor* M145 as detailed in the Materials and Methods section. The +25 to +696 region of *ylmE* (SCO2080) or the +25 to +705 region of *ylmD* (SCO2081) were replaced by the apramycin resistance cassette, followed by deletion of the cassette using the Cre recombinase so as to avoid polar effects. For each mutant, four independent mutants were selected and all had the same phenotype. Therefore, one was selected for more detailed analysis, designated GAL47 (*S. coelicolor* M145 Δ*ylmD*) and GAL48 (*S. coelicolor* M145 Δ*ylmE*).

The *ylmD* null mutant GAL47 had a light grey appearance, while *ylmE* null mutant GAL48 hardly produced any grey pigment after 6 days incubation. The lack of grey-pigmented spores is indicative of a failure to complete full development (Fig. 2A). Phase-contrast light microscopy of impression prints of the top of the colonies demonstrated that while the parent produced typical long spore chains, the *ylmD* null mutant produced many aberrantly sized (and in particular large) spores, while the *ylmE* null mutant produced fewer spores and those produced were unusually large. The same defect in sporulation was observed on R5 and MM mannitol agar plates. Antibiotic production was not affected, and the mutants produced normal levels of the pigmented antibiotics actinorhodin and undecylprodigiosin. To further ascertain that the sporulation defects were indeed solely due to the deletion of the respective genes, we introduced plasmids expressing *ylmD* or *ylmD-egfp* in the in the *ylmD* null mutant and *ylmE* or *ylmE-egfp* in the *ylmE* mutant, in all cases with transcription directed from the native *ftsZ* promoter region. While the majority of the spores of the complemented *ylmD* mutant had a regular appearance, those of the complemented *ylmE* mutants still showed variable lengths (Fig. 2B). This partial complementation suggests that the deletion of *ylmE* may have polar effect on the expression of its downstream genes. This is supported by the fact that introduction of a plasmid harbouring the entire region from *ftsZ* to *divIVA* fully restored sporulation to *ylmE* mutants (Fig. S1).

To study the spores of *ylmD* and *ylmE* null mutants at high resolution, cryo-scanning electron microscopy (SEM) was performed, which again demonstrated the sporulation defects. The parental strain *S. coelicolor* M145 produced abundant spore chains, with nearly all hyphae fully developed into mature spore chains (Fig. 3AB). The *ylmD* null mutant GAL47 frequently

produced aberrantly sized spores (Fig. 3CD), while in *ylmE* null mutant GAL48, precious few and often aberrant spores were identified (Fig. 3EF). Mutants were also created in *Streptomyces lividans* 66, and these again showed the same morphology, strongly supporting the notion that the observed phenotypes were solely due to the mutations in *ylmD* or *ylmE* (data not shown). The highly similar phenotypes of the *S. coelicolor* and *S. lividans* mutants support the notion that the genes play a key role in sporulation-specific cell division and are consistent with the conserved function of the genes in sporulation-specific cell division in *Streptomyces*.

Deletion of *ylmD* and *ylmE* results in aberrant morphology and reduced viability of spores

Viability of the spores was tested by plating around 1000 spores - counted in a haemocytometer - of *S. coelicolor* M145 and its mutants GAL47 (Δ*ylm*D) and GAL48 (Δ*ylmE*) onto SFM agar plates. While the wild-type strain had close to 100% viability, spores of the *ylmD* and *ylmE* mutants had reduced viability, with 50% and 60% viable spores, respectively. Spores of in particular the *ylmE* mutant were also more heat sensitive, with 24% viability after 5 min incubation at 60^0C, as compared to 44% survival for *ylmD* null mutant spores and 50% for the wild-type strain.

To analyze the possible cell wall defects in more detail, all strains were grown on SFM agar plates for 5 days and analysed by Transmission Electron Microscopy (TEM) (Fig. 4). The parent produced typical spore chains and thick-walled spores. Conversely, *ylmD* and *ylmE* mutant spores were deformed and highly irregular. In particular the spores of the *ylmE* mutant had a thin wall similar to that of hyphae, suggesting that spore-wall synthesis was compromised.

YlmD and YlmE are required for peptidoglycan synthesis at the septum

To analyze cell wall and membrane distribution in *ylmD* and *ylmE* mutants, fluorescence microscopy was performed on two-days old SFM surface-grown cultures of mutants GAL47 (M145 Δ*ylmD*) and GAL48 (M145 Δ*ylmE*) and compared to the parental strain M145. Peptidoglycan precursors were stained with FITC-WGA or Oregon-WGA and membranes visualized by staining with FM5-95. In wild-type pre-division aerial hyphae, long symmetrical septal ladders were observed when stained for cell wall or membranes (Fig. 5A). In contrast, aerial hyphae of the mutants showed highly disturbed cell wall and membrane distribution, which was more pronounced in *ylmE* than in *ylmD* mutants (Fig. 5AB). The *ylmE* mutants were mostly devoid of septation, which could be complemented via re-introduction of *ylmE*; similarly, septation was restored to the *ylmE* mutant by re-introduction of *ylmE*, although peptidoglycan synthesis and septum spacing was still irregular (Fig. 5C). These data suggest an important role for YlmD and in particular YlmE in cell-wall synthesis during sporulation.

Cellular localization of YlmD and YlmE

Given the impact of *ylmDE* on sporulation, we analysed how YlmD and YlmE were localized in the hyphae of *S. coelicolor*. To this end, constructs based on the low-copy number vector pHJL401 were prepared to allow the expression of YlmD-eGFP and YlmE-eGFP fusion proteins, which were expressed from the natural *ftsZ* promoter region (see Materials and Methods section for details). These constructs were then introduced into *S. coelicolor* M145 and (as a control for functionality) in the mutants. The constructs partially restored development to the respective mutants, with significant restoration of the sporulation defects in *ylmD* mutants, and partial restoration of sporulation to *ylmE* mutants (Fig. 2B). Both YlmD-eGFP and YlmE-eGFP

mostly showed diffuse localization along the wall of the aerial hyphae and in spores of *S. coelicolor* M145 (Fig. 6). During early stages of sporulation, fluorescence became more intense, indicative of increased expression of the proteins (Fig. 6). During later stages of sporulation, YlmD-eGFP and YlmE-eGFP showed an irregular pattern of varying intensity, with some spores showing bright fluorescence indicative of high concentrations of YlmD or YlmE, while others hardly showed any fluorescence (Fig 6). This suggests that YlmD and YlmE are differentially expressed throughout nascent spore chains, and do not exclusively co-localise with FtsZ and the divisome.

Localization of FtsZ is disturbed in *ylmD* and *ylmE* null mutants

To investigate the localization of FtsZ in the mutants, integrative plasmid pKF41 that expresses FtsZ-eGFP from the native *ftsZ* promoter region (Grantcharova *et al.*, 2005) was introduced into the *ylmD* and *ylmE* mutants, to generate strain GAL52 and GAL53, respectively. Prior to sporulation, typical ladders of Z-rings were observed in the parental strain *S. coelicolor* M145, while *ylmD* and *ylmE* null mutants showed abnormal Z-ladders (Fig. 7). In the absence of YlmD, ladders were still observed, but the intensity varied and spacing between the individual rings was far less regular, with many neighboring Z-rings either close together or widely spaced. Consistent with the sporulation defect, *ylmE* null mutants produced very few Z-rings, and the few Z-ladders that where formed were highly irregular or unfinished, and significantly shorter than in the parental strain. Thus, FtsZ localization is irregular in *ylmD* mutants and highly compromised in *ylmE* mutants, consistent with a role for YlmE and to a lesser extent YlmD in (the control of) sporulation-specific cell division.

CONCLUSIONS

Phylogenetic analysis shows strong linkage between *ylmD*, *ylmE* and *ftsZ,* and this is further validated by the transcriptional organization, with the three genes forming a single transcription unit in streptomycetes. All bacteria that have *ylmD* also have *ylmE*, while conversely, *ylmD* is often lost in strains that have retained *ylmE*. This suggests that is unlikely that YlmD is solely required for the proper function of YlmE. In line with this, *ylmE* plays a key role in sporulation-specific cell division, while *ylmD* appears less important. Mutants lacking *ylmE* have a severe phenotype, with highly compromised cell-wall synthesis, and aberrant division. Mutants that lacked *ylmD* produced abundant spores, but with aberrant shapes and variable lengths. FtsZ-ladders were seen in sporogenic aerial hyphae of *ylmD* mutants, although with imperfect symmetry, while FtsZ failed to localise properly in *ylmE* mutants. Taken together, the racemase-like protein YlmE plays an important role in (the control of) sporulation-specific cell division in streptomycetes, supported by YlmD. We are currently performing detailed structural and functional analysis of these proteins, to elucidate their precise role in bacterial cell division.

MATERIALS AND METHODS

Phylogenetic analysis of *ylmD* and *ylmE*

The amino acid sequence of YlmD and YlmE were extracted from StreptDB (http://strepdb.streptomyces.org.uk) and used to search the NCBI database (www.ncbi.nlm.nih.gov) using BLASTP against the non-redundant protein sequence database. Alignment of YlmD and YlmE was generated using ClustalW (Thompson *et al.*, 1994) followed by

manual editing in MEGA v. 4.0. The neighbour-joining trees (Saitou and Nei, 1987) were generated with default parameters settings as implemented in MEGA v. 4.0 (Tamura *et al.*, 2007). The maximum-likelihood trees were made using the best fit models predicted by MEGA. Tree reliability was estimated by bootstrapping with 1000 replicates. Trees were drawn with either N-J or ML algorithms gave trees of similar topologies indicating that the phylogenies are likely to reliable.

Bacterial strains and media

All bacterial strains used in this study are listed in Table S1. *E. coli* JM109 was used for routine cloning and ET12567 (MacNeil *et al.*, 1992) to prepare nonmethylated DNA to bypass the methyl-specific restriction system of *S. coelicolor*. *E. coli* strains were propagated in Luria broth, where appropriate supplemented with antibiotics for selection, namely ampicillin (100 µg/ml end concentration), apramycin (50 µg/ml) and/or chloramphenicol (25 µg/ml). *S. coelicolor* A3(2) M145 (Bentley *et al.*, 2002) and *S. lividans* 66 (Cruz-Morales *et al.*, 2013) were obtained from the John Innes Centre strain collection. *S. coelicolor* strains were grown on soya flour medium (SFM) or minimal media mannitol (MM) agar plates for phenotypic characterization and on R5 agar plates for regeneration of protoplasts (Kieser *et al.*, 2000). Antibiotics used for screening Streptomyces were apramycin (20 µg/ml end concentration) and thiostrepton (10 µg/ml).

Plasmids and constructs

All plasmids and constructs described in this study are summarized in Table S2. The oligonucleotides used for PCR are listed in Table S3. PCR reactions were performed using Pfu DNA polymerase as described (Colson *et al.*, 2007).

Constructs for the deletion of ylmD and ylmE

The strategy for creating knock-out mutants is based on the unstable multi-copy vector pWHM3 (Vara *et al.*, 1989) as described previously (Świątek *et al.*, 2012). For each knock-out construct roughly 1.5 kb of upstream and downstream region of the respective genes were amplified by PCR from cosmid St4A10 that contains the *dcw* cluster of *S. coelicolor*. The upstream region was thereby cloned as an EcoRI-XbaI fragment, and the downstream part as an XbaI-BamHI fragment , and these were ligated into EcoRI-BamHI-digested pWHM3 (for the precise location of the oligonucleotides see Table S3). In this way, an XbaI site was engineered in-between the flanking regions of the gene of interest. This was then used to insert the apramycin resistance cassette *aac(3)IV* flanked by *loxP* sites, using engineered XbaI sites. The presence of the *loxP* recognition sites allows the efficient removal of the apramycin resistance cassette following the introduction of a plasmid pUWL-Cre expressing the Cre recombinase (Fedoryshyn *et al.*, 2008; Khodakaramian *et al.*, 2006). Knock-out plasmids pGWS728 and pGWS729 were created for the deletion of nucleotide positions +25/+696 of *ylmE* (SCO2080) and +25/+705 of *ylmD* (SCO2081), whereby +1 refers to the translational start site of the respective genes. This allowed first the replacement by the apramycin resistance cassette. Subsequently the apramycin resistance cassette was removed using expression of pUWLCre.

For complementation of the *ylmE* and *ylmD* null mutants, the entire coding regions of SCO2080 and SCO2081 (with stop codons) were amplified from the *S. coelicolor* M145 chromosome using primer pairs ylmE_F+1 and ylmE_R+723 and ylmD_F+1 and ylmD_R+732, respectively. The PCR products were digested with StuI/XbaI, and inserted downstream of the native *ftsZ* promoter region in pHJL401, respectively. Thus constructs pGWS1042 and pGWS1043 were generated that express *ylmE* and *ylmD*, respectively, under control of the *S. coelicolor ftsZ* promoter region.

Alternatively, construct pKR8 (Ramijan *et al.*, 2016) was used for complementation; pKR8 is based on integrative vector pIJ8600 (Sun *et al.*, 1999) and contains the 2227742-2241015 region of the *S. coelicolor* genome, encompassing the end of *murX* (SCO2087), the entire coding sequences of *murD, ftsW, murG, ftsQ, ftsZ, ylmD, ylmE, sepF, sepG, divIVA* and a large part of SCO2076 (encoding Ile-tRNA synthetase).

Constructs for the localization of YlmD and YlmE

The entire coding regions of SCO2080 and SCO2081 (without stop codons) were amplified from the *S. coelicolor* M145 chromosome using primer pairs ylmE_F+1 and ylmE_R+717 and ylmD_F+1 and ylmD_R+726, respectively. The PCR products were digested with StuI/BamHI, and inserted downstream of the native *ftsZ* promoter region and immediately upstream of *egfp* in pHJL401. The latter is a highly stable vector with low copy number that generally results in wild-type transcription levels and is well suited for among others complementation experiments (van Wezel *et al.*, 2000b). Thus constructs pGWS757 and pGWS758 were generated that express YlmE-eGFP and YlmD-eGFP, respectively, from the native *S. coelicolor ftsZ* promoter region.

Plasmid pKF41 expresses FtsZ-eGFP from its own promoter region (Grantcharova *et al.*, 2005). Constructs pGWS757 and pGWS758 were also used to complement *ylmE* and *ylmD* null mutants, respectively.

Microscopy

Fluorescence and light microscopy were performed as described previously (Willemse and van Wezel, 2009). For peptidoglycan staining we used FITC-labeled wheat germ agglutinin (FITC-WGA) or Oregon Green 488 conjugated WGA (Oregon-WGA); for membrane staining, we used FM5-95 (all obtained from Molecular Probes). All images were background-corrected, setting the signal outside the hyphae to 0 to obtain a sufficiently dark background. These corrections were made using Adobe Photoshop CS4. Cryo-scanning electron microscopy (cryo-SEM) and transmission electron microscopy (TEM) were performed as described (Piette *et al.*, 2005).

Computer analysis

DNA and protein database searches were completed by using StrepDB page (http://strepdb.streptomyces.org.uk/). Phylogenetic analysis was done using the STRING engine at EMBL (www.string.EMBL).

Acknowledgements

This work was supported by the Netherlands Organization for Scientific Research (NWO), via VICI grant 10379 to GPvW. The authors declare no conflict of interests.

REFERENCES

Adams, D.W., and Errington, J. (2009) Bacterial cell division: assembly, maintenance and disassembly of the Z ring. *Nat Rev Microbiol* **7**: 642-653.

Barka, E.A., Vatsa, P., Sanchez, L., Gavaut-Vaillant, N., Jacquard, C., Meier-Kolthoff, J., Klenk, H.P., Clément, C., Oudouch, Y., and van Wezel, G.P. (2016) Taxonomy, physiology, and natural products of the *Actinobacteria*. *Microbiol Mol Biol Rev* **80**: 1-43.

Bentley, S.D., Chater, K.F., Cerdeno-Tarraga, A.M., Challis, G.L., Thomson, N.R., James, K.D., Harris, D.E., Quail, M.A., Kieser, H., Harper, D., Bateman, A., Brown, S., Chandra, G., Chen, C.W., Collins, M., Cronin, A., Fraser, A., Goble, A., Hidalgo, J., Hornsby, T., Howarth, S., Huang, C.H., Kieser, T., Larke, L., Murphy, L., Oliver, K., O'Neil, S., Rabbinowitsch, E., Rajandream, M.A., Rutherford, K., Rutter, S., Seeger, K., Saunders, D., Sharp, S., Squares, R., Squares, S., Taylor, K., Warren, T., Wietzorrek, A., Woodward, J., Barrell, B.G., Parkhill, J., and Hopwood, D.A. (2002) Complete genome sequence of the model actinomycete *Streptomyces coelicolor* A3(2). *Nature* **417**: 141-147.

Bi, E.F., and Lutkenhaus, J. (1991) FtsZ ring structure associated with division in *Escherichia coli*. *Nature* **354**: 161-164.

Celler, K., Koning, R.I., Koster, A.J., and van Wezel, G.P. (2013) Multidimensional view of the bacterial cytoskeleton. *J Bacteriol* **195**: 1627-1636.

Celler, K., Koning, R.I., Willemse, J., Koster, A.J., and van Wezel, G.P. (2016) Cross-membranes orchestrate compartmentalization and morphogenesis in *Streptomyces*. *Nat Comm* **7**: 11836.

Claessen, D., Rozen, D.E., Kuipers, O.P., Sogaard-Andersen, L., and van Wezel, G.P. (2014) Bacterial solutions to multicellularity: a tale of biofilms, filaments and fruiting bodies. *Nat Rev Microbiol* **12**: 115-124.

Claus, H. (2003) Laccases and their occurrence in prokaryotes. *Arch Microbiol* **179**: 145-150.

Colson, S., Stephan, J., Hertrich, T., Saito, A., van Wezel, G.P., Titgemeyer, F., and Rigali, S. (2007) Conserved *cis*-acting elements upstream of genes composing the chitinolytic system of streptomycetes are DasR-responsive elements. *J Mol Microbiol Biotechnol* **12**: 60-66.

Cruz-Morales, P., Vijgenboom, E., Iruegas-Bocardo, F., Girard, G., Yanez-Guerra, L.A., Ramos-Aboites, H.E., Pernodet, J.L., Anne, J., van Wezel, G.P., and Barona-Gomez, F. (2013) The genome sequence of *Streptomyces lividans* 66 reveals a novel tRNA-dependent peptide biosynthetic system within a metal-related genomic island. *Genome Biol Evol* **5**: 1165-1175.

Eswaramoorthy, S., Gerchman, S., Graziano, V., Kycia, H., Studier, F.W., and Swaminathan, S. (2002) Structure of a yeast hypothetical protein selected by a structural genomics approach. *Acta Crystallogr D Biol Crystallogr* **59**: 127-135.

Fedoryshyn, M., Welle, E., Bechthold, A., and Luzhetskyy, A. (2008) Functional expression of the Cre recombinase in actinomycetes. *Appl Microbiol Biotechnol* **78**: 1065-1070.

Flärdh, K., and Buttner, M.J. (2009) *Streptomyces* morphogenetics: dissecting differentiation in a filamentous bacterium. *Nat Rev Microbiol* **7**: 36-49.

Girard, G., Traag, B.A., Sangal, V., Mascini, N., Hoskisson, P.A., Goodfellow, M., and van Wezel, G.P. (2013) A novel taxonomic marker that discriminates between morphologically complex actinomycetes. *Open Biology* **3**.

Goehring, N.W., and Beckwith, J. (2005) Diverse paths to midcell: assembly of the bacterial cell division machinery. *Curr Biol* **15**: R514-526.

Grantcharova, N., Lustig, U., and Flärdh, K. (2005) Dynamics of FtsZ assembly during sporulation in *Streptomyces coelicolor* A3(2). *Journal of bacteriology* **187**: 3227-3237.

Gueiros-Filho, F.J., and Losick, R. (2002) A widely conserved bacterial cell division protein that promotes assembly of the tubulin-like protein FtsZ. *Genes Dev* **16**: 2544-2556.

Hale, C.A., and de Boer, P.A.J. (1997) Direct Binding of FtsZ to ZipA, an essential component of the septal ring structure that mediates cell division in *E. coli. Cell* **88**: 175-185.

Hamoen, L.W., Meile, J.C., de Jong, W., Noirot, P., and Errington, J. (2006) SepF, a novel FtsZ-interacting protein required for a late step in cell division. *Mol Microbiol* **59**: 989-999.

Holmes, N.A., Walshaw, J., Leggett, R.M., Thibessard, A., Dalton, K.A., Gillespie, M.D., Hemmings, A.M., Gust, B., and Kelemen, G.H. (2013) Coiled-coil protein Scy is a key component of a multiprotein assembly controlling polarized growth in *Streptomyces*. *Proc Natl Acad Sci U S A* **110**: E397-406.

Hopwood, D.A. (2007) *Streptomyces in nature and medicine: the antibiotic makers.* New York: Oxford University Press.

Ishikawa, S., Kawai, Y., Hiramatsu, K., Kuwano, M., and Ogasawara, N. (2006) A new FtsZ-interacting protein, YlmF, complements the activity of FtsA during progression of cell division in *Bacillus subtilis*. *Mol Microbiol* **60**: 1364-1380.

Jakimowicz, D., and van Wezel, G.P. (2012) Cell division and DNA segregation in *Streptomyces*: how to build a septum in the middle of nowhere? *Mol Microbiol* **85**: 393-404.

Keijser, B.J., Noens, E.E., Kraal, B., Koerten, H.K., and van Wezel, G.P. (2003) The *Streptomyces coelicolor ssgB* gene is required for early stages of sporulation. *FEMS Microbiol Lett* **225**: 59-67.

Khodakaramian, G., Lissenden, S., Gust, B., Moir, L., Hoskisson, P.A., Chater, K.F., and Smith, M.C.M. (2006) Expression of Cre recombinase during transient phage infection permits efficient marker removal in *Streptomyces*. *Nucleic Acids Res* **34**: e20.

Kieser, T., Bibb, M.J., Buttner, M.J., Chater, K.F., and Hopwood, D.A. (2000) *Practical Streptomyces genetics.*: John Innes Foundation.

MacNeil, D.J., Gewain, K.M., Ruby, C.L., Dezeny, G., Gibbons, P.H., and Maeneil, T. (1992) Analysis of *Streptomyces avermitilis* genes required for avermectin biosynthesis utilizing a novel integration vector. *Gene* **111**: 61-68.

McCormick, J.R., Su, E.P., Driks, a., and Losick, R. (1994) Growth and viability of *Streptomyces coelicolor* mutant for the cell division gene *ftsZ*. *Mol Microbiol* **14**: 243-254.

McCormick, J.R., and Losick, R. (1996) Cell division gene *ftsQ* is required for efficient sporulation but not growth and viability in *Streptomyces coelicolor* A3(2). *J Bacteriol* **178**: 5295-5301.

McCormick, J.R. (2009) Cell division is dispensable but not irrelevant in *Streptomyces*. *Curr Opin Biotechnol* **12**: 689-698.

Mingorance, J., Tamames, J., and Vicente, M. (2004) Genomic channeling in bacterial cell division. *J Mol Recognit* **17**: 481-487.

Percudani, R., and Peracchi, A. (2003) A genomic overview of pyridoxal-phosphate-dependent enzymes. *EMBO R* **4**: 850-854.

Pichoff, S., and Lutkenhaus, J. (2002) Unique and overlapping roles for ZipA and FtsA in septal ring assembly in *Escherichia coli*. *EMBO J* **21**: 685-693.

Piette, A., Derouaux, A., Gerkens, P., Noens, E.E., Mazzucchelli, G., Vion, S., Koerten, H.K., Titgemeyer, F., De Pauw, E., Leprince, P., van Wezel, G.P., Galleni, M., and Rigali, S. (2005) From dormant to germinating spores of *Streptomyces coelicolor* A3(2): new perspectives from the *crp* null mutant. *J Proteome Res* **4**: 1699-1708.

RayChaudhuri, D. (1999) ZipA is a MAP-Tau homolog and is essential for structural integrity of the cytokinetic FtsZ ring during bacterial cell division. *EMBO J* **18**: 2372-2383.

Romberg, L., and Levin, P.A. (2003) Assembly dynamics of the bacterial cell division protein FtsZ: poised at the edge of stability. *Annu Rev Microbiol* **57**: 125-154.

Romero, D.A., Hasan, A.H., Lin, Y.F., Kime, L., Ruiz-Larrabeiti, O., Urem, M., Bucca, G., Mamanova, L., Laing, E.E., van Wezel, G.P., Smith, C.P., Kaberdin, V.R., and McDowall, K.J. (2014) A comparison of key aspects of gene regulation in *Streptomyces coelicolor* and *Escherichia coli* using nucleotide-resolution transcription maps produced in parallel by global and differential RNA sequencing. *Mol Microbiol*.

Saitou, N., and Nei, M. (1987) The neighbor-joining method: a new method for reconstructing phylogenetic trees. *Mol Biol Evol* **4**: 406-425.

Schwedock, J., McCormick, J.R., Angert, E.R., Nodwell, J.R., and Losick, R. (1997) Assembly of the cell division protein FtsZ into ladder like structures in the aerial hyphae of *Streptomyces coelicolor*. *Mol Microbiol* **25**: 847-858.

Sun, J., Kelemen, G.H., Fernandez-Abalos, J.M., and Bibb, M.J. (1999) Green fluorescent protein as a reporter for spatial and temporal gene expression in *Streptomyces coelicolor* A3(2). *Microbiology* **145**: 2221-2227.

Swiatek, M.A., Gubbens, J., Bucca, G., Song, E., Yang, Y.H., Laing, E., Kim, B.G., Smith, C.P., and van Wezel, G.P. (2013) The ROK family regulator Rok7B7 pleiotropically affects xylose utilization, carbon catabolite repression, and antibiotic production in *Streptomyces coelicolor*. *J Bacteriol* **195**: 1236-1248.

Świątek, M.A., Tenconi, E., Rigali, S., and van Wezel, G.P. (2012) Functional analysis of the N-acetylglucosamine metabolic genes of *Streptomyces coelicolor* and role in control of development and antibiotic production. *Journal of bacteriology* **194**: 1136-1144.

Szklarczyk, D., Franceschini, A., Kuhn, M., Simonovic, M., Roth, A., Minguez, P., Doerks, T., Stark, M., Muller, J., Bork, P., Jensen, L.J., and von Mering, C. (2011) The STRING database in 2011: functional interaction networks of proteins, globally integrated and scored. *Nucleic Acids Res* **39**: D561-D568.

Tamura, K., Dudley, J., Nei, M., and Kumar, S. (2007) MEGA4: Molecular Evolutionary Genetics Analysis (MEGA) software version 4.0. *Mol Biol Evol* **24**: 1596-1599.

Tassoni, R., van der Aart, L.T., Ubbink, M., van Wezel, G.P., and Pannu, N.S. (2017) Structural and functional characterization of the alanine racemase from *Streptomyces coelicolor* A3(2). *Biochem Biophys Res Commun* **483**: 122-128.

Thompson, J.D., Higgins, D.G., and Gibson, T.J. (1994) Clustal-W - Improving the Sensitivity of Progressive Multiple Sequence Alignment through Sequence Weighting, Position-Specific Gap Penalties and Weight Matrix Choice. *Nucleic Acids Res* **22**: 4673-4680.

Traag, B.A., and van Wezel, G.P. (2008) The SsgA-like proteins in actinomycetes: small proteins up to a big task. *Antonie Van Leeuwenhoek* **94**: 85-97.

van Wezel, G.P., van der Meulen, J., Kawamoto, S., Luiten, R.G., Koerten, H.K., and Kraal, B. (2000a) *ssgA* is essential for sporulation of *Streptomyces coelicolor* A3(2) and affects hyphal development by stimulating septum formation. *J Bacteriol* **182**: 5653-5662.

van Wezel, G.P., White, J., Hoogvliet, G., and Bibb, M.J. (2000b) Application of *redD*, the transcriptional activator gene of the undecylprodigiosin biosynthetic pathway, as a reporter for transcriptional activity in *Streptomyces coelicolor* A3(2) and *Streptomyces lividans*. *J Mol Microbiol Biotechnol* **2**: 551-556.

Vara, J., Lewandowska-Skarbek, M., Wang, Y.G., Donadio, S., and Hutchinson, C.R. (1989) Cloning of genes governing the deoxysugar portion of the erythromycin biosynthesis pathway in *Saccharopolyspora erythraea* (*Streptomyces erythreus*). *Journal of bacteriology* **171**: 5872-5881.

Wildermuth, H., and Hopwood, D. (1970) Septation during sporulation in *Streptomyces coelicolor. J Gen Microbiol* **60**: 51-59.

Willemse, J., and van Wezel, G.P. (2009) Imaging of *Streptomyces coelicolor* A3(2) with Reduced Autofluorescence Reveals a Novel Stage of FtsZ Localization. *PLoS ONE* **4**: e4242.

Willemse, J., Borst, J.W., de Waal, E., Bisseling, T., and van Wezel, G.P. (2011) Positive control of cell division: FtsZ is recruited by SsgB during sporulation of *Streptomyces*. *Genes Dev* **25**: 89-99.

Yagüe, P., Willemse, J., Koning, R.I., Rioseras, B., Lopez-Garcia, M.T., Gonzalez-Quinonez, N., Lopez-Iglesias, C., Shliaha, P.V., Rogowska-Wrzesinska, A., Koster, A.J., Jensen, O.N., van Wezel, G.P., and Manteca, A. (2016) Subcompartmentalization by cross-membranes during early growth of *Streptomyces* hyphae. *Nat Commun* **7**: 12467.

Zhang, L., Willemse, J., Claessen, D., and van Wezel, G.P. (2016) SepG coordinates sporulation-specific cell division and nucleoid organization in *Streptomyces coelicolor*. *Open Biol* **6**: 150164.

FIGURE LEGENDS

Figure 1. Phylogenetic analysis of YlmE in actinobacteria and its genetic linkage to *ylmD*. A phylogenetic tree is shown of YlmE in actinobacteria (left) and genetic linkage of *ylmE* (grey) to *ftsZ* (black) and *ylmD* (white) (right).

Figure 2. Phenotype of the *S. coelicolor ylmD* and *ylmE* mutants. (A) sporulation of *S. coelicolor* M145 and its *ylmD* and *ylmE* mutants on SFM agar. Note the lack of grey pigmentation of the *ylmE* mutant, indicative of a sporulation defect. (B) phase-contrast micrographs of impression prints of the strains shown in (A) as well as the complemented mutants. Arrows point at irregularly shaped spores in the *ylmD* mutant. The sporulation defect of the *ylmD* mutant could be complemented by introduction of wild-type *ylmD* and *ylmD-eGFP*, while complementation of the *ylmE* mutant by wild-type *ylmE* or *ylmE-egfp* restored sporulation, although irregularly sized spores were often produced. Bar, 5 µm.

Figure 3. Cryo-scanning electron micrographs of aerial hyphae of *S. coelicolor* M145 and its *ylmD* and *ylmE* mutants. The parental strain produced wild-type spores, the *ylmD* mutant produced abundant but often irregular spores, while the *ylmE* null mutant produced occasional spores with highly irregular sizes. Cultures were grown on SFM agar plates for 5 days at 30^0C. Bars: top row, 1 µm; bottom row, 5 µm.

Figure 4. Transmission electron micrographs of spores of *S. coelicolor* M145 and its *ylmD* and *ylmE* mutants. Wild-type spores (M145) show regular sizes and appearance (A). In contrast, spores of the *ylmD* (B) and *ylmE* (C) null mutants have an irregular appearance. Note the lighter appearance of the spore wall in the *ylmD* null mutant and the lack of the typical thick spore wall in *ylmE* mutants. Cultures were grown on SFM agar plates for 5 days at 30^0C. Bar, 500 nm.

Figure 5. Fluorescence microscopy of cell wall, DNA and membranes.

(A) Fluorescent micrographs of hyphae stained for cell-wall synthesis (FITC-WGA or Oregon-WGA) or membranes (FM5-95). An overlay of these images is presented in the third column, and the corresponding light image in the last column. Bar, 5 µm. (B) close-ups of the composite images of 5A. Bar, 5 µm. (C) Fluorescence micrographs showing DNA and cell-wall distribution in the complemented *ylmD* and *ylmE* mutants. While ladders of septa were formed in both strains, indicative that sporulation was restored to the mutants, in particular the complemented *ylmE* mutant formed imperfect septa. Bar, 10 µm.

Figure 6. Localization of YlmD-GFP and YlmE-GFP. Sporogenic aerial hyphae of *S. coelicolor* M145 at different stages of development were imaged by fluorescence microscopy visualizing YlmD-eGFP and YlmE-eGFP. Stages were: early aerial development, late aerial development and sporulation maturation. During sporulation, YlmD had a 'patchy' localization, while YlmE was frequently seen to localize in a ring-like fashion inside the spores, suggesting that at this stage YlmD and YlmE may co-localize with the cell-wall synthetic machinery. Bar, 5 µm.

Figure 7. Localization of FtsZ-eGFP in *S. coelicolor* M145 and its *ylmD* and *ylmE* mutants. FtsZ-eGFP formed typical ladders in wild-type cells (M145). In contrast, YlmE is required for the formation of ladders of FtsZ, while the absence of YlmD caused irregular spacing between the septa. Cultures were grown on SFM agar plates for 5 days at 30^0C. Bar, 5 µm.

Figure 1

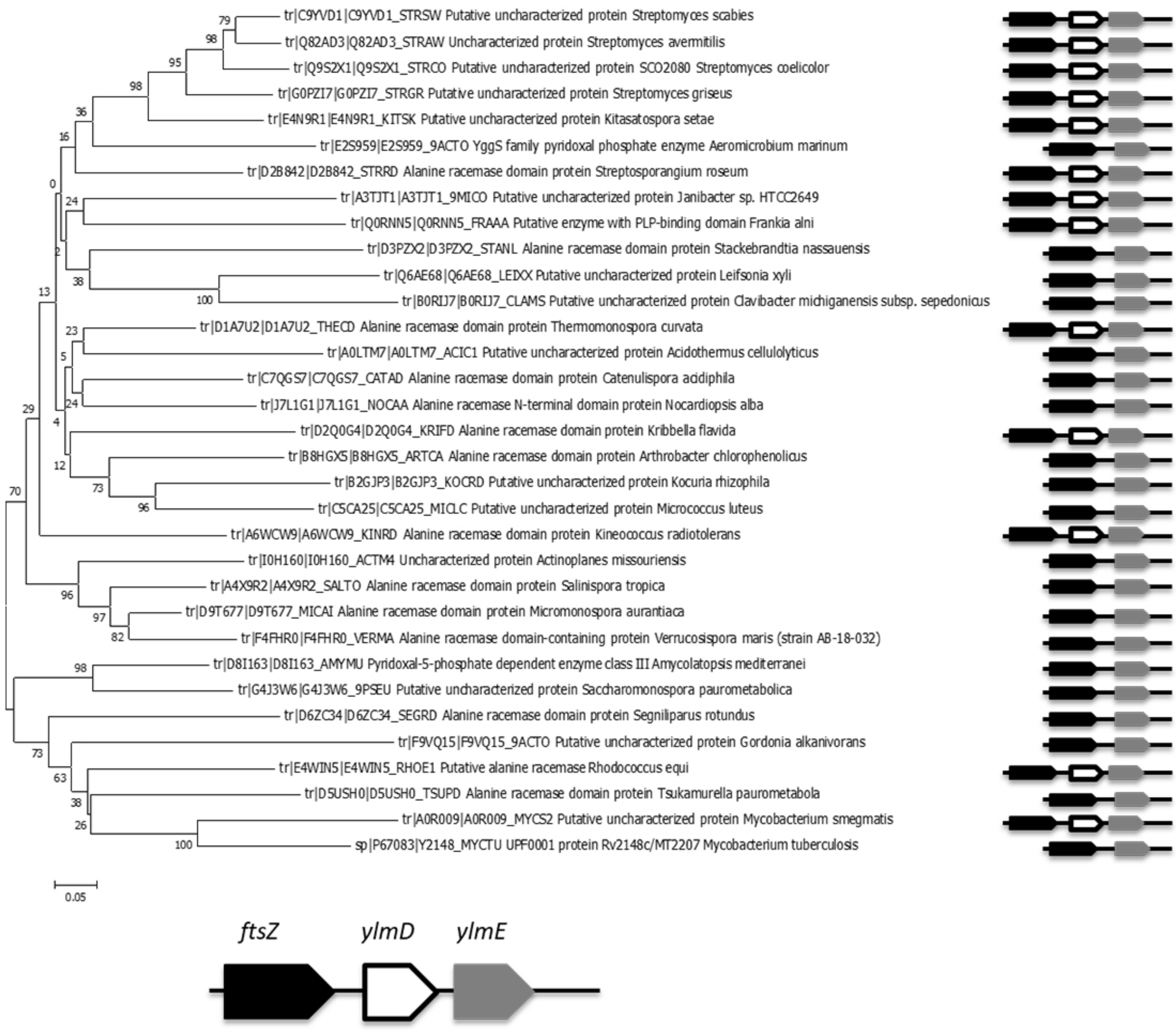
tr|C9YVD1|C9YVD1_STRSW Putative uncharacterized protein Streptomyces scabies
tr|Q82AD3|Q82AD3_STRAW Uncharacterized protein Streptomyces avermitilis
tr|Q9S2X1|Q9S2X1_STRCO Putative uncharacterized protein SCO2080 Streptomyces coelicolor
tr|G0PZI7|G0PZI7_STRGR Putative uncharacterized protein Streptomyces griseus
tr|E4N9R1|E4N9R1_KITSK Putative uncharacterized protein Kitasatospora setae
tr|E2S959|E2S959_9ACTO YggS family pyridoxal phosphate enzyme Aeromicrobium marinum
tr|D2B842|D2B842_STRRD Alanine racemase domain protein Streptosporangium roseum
tr|A3TJT1|A3TJT1_9MICO Putative uncharacterized protein Janibacter sp. HTCC2649
tr|Q0RNN5|Q0RNN5_FRAAA Putative enzyme with PLP-binding domain Frankia alni
tr|D3PZX2|D3PZX2_STANL Alanine racemase domain protein Stackebrandtia nassauensis
tr|Q6AE68|Q6AE68_LEIXX Putative uncharacterized protein Leifsonia xyli
tr|B0RIJ7|B0RIJ7_CLAMS Putative uncharacterized protein Clavibacter michiganensis subsp. sepedonicus
tr|D1A7U2|D1A7U2_THECD Alanine racemase domain protein Thermomonospora curvata
tr|A0LTM7|A0LTM7_ACIC1 Putative uncharacterized protein Acidothermus cellulolyticus
tr|C7QGS7|C7QGS7_CATAD Alanine racemase domain protein Catenulispora acidiphila
tr|J7L1G1|J7L1G1_NOCAA Alanine racemase N-terminal domain protein Nocardiopsis alba
tr|D2Q0G4|D2Q0G4_KRIFD Alanine racemase domain protein Kribbella flavida
tr|B8HGX5|B8HGX5_ARTCA Alanine racemase domain protein Arthrobacter chlorophenolicus
tr|B2GJP3|B2GJP3_KOCRD Putative uncharacterized protein Kocuria rhizophila
tr|C5CA25|C5CA25_MICLC Putative uncharacterized protein Micrococcus luteus
tr|A6WCW9|A6WCW9_KINRD Alanine racemase domain protein Kineococcus radiotolerans
tr|I0H160|I0H160_ACTM4 Uncharacterized protein Actinoplanes missouriensis
tr|A4X9R2|A4X9R2_SALTO Alanine racemase domain protein Salinispora tropica
tr|D9T677|D9T677_MICAI Alanine racemase domain protein Micromonospora aurantiaca
tr|F4FHR0|F4FHR0_VERMA Alanine racemase domain-containing protein Verrucosispora maris (strain AB-18-032)
tr|D8I163|D8I163_AMYMU Pyridoxal-5-phosphate dependent enzyme class III Amycolatopsis mediterranei
tr|G4J3W6|G4J3W6_9PSEU Putative uncharacterized protein Saccharomonospora paurometabolica
tr|D6ZC34|D6ZC34_SEGRD Alanine racemase domain protein Segniliparus rotundus
tr|F9VQ15|F9VQ15_9ACTO Putative uncharacterized protein Gordonia alkanivorans
tr|E4WIN5|E4WIN5_RHOE1 Putative alanine racemase Rhodococcus equi
tr|D5USH0|D5USH0_TSUPD Alanine racemase domain protein Tsukamurella paurometabola
tr|A0R009|A0R009_MYCS2 Putative uncharacterized protein Mycobacterium smegmatis
sp|P67083|Y2148_MYCTU UPF0001 protein Rv2148c/MT2207 Mycobacterium tuberculosis
0.05
ftsZ
ylmD
ylmE

Figure 2

A

M145
ΔylmD
ΔylmE

B

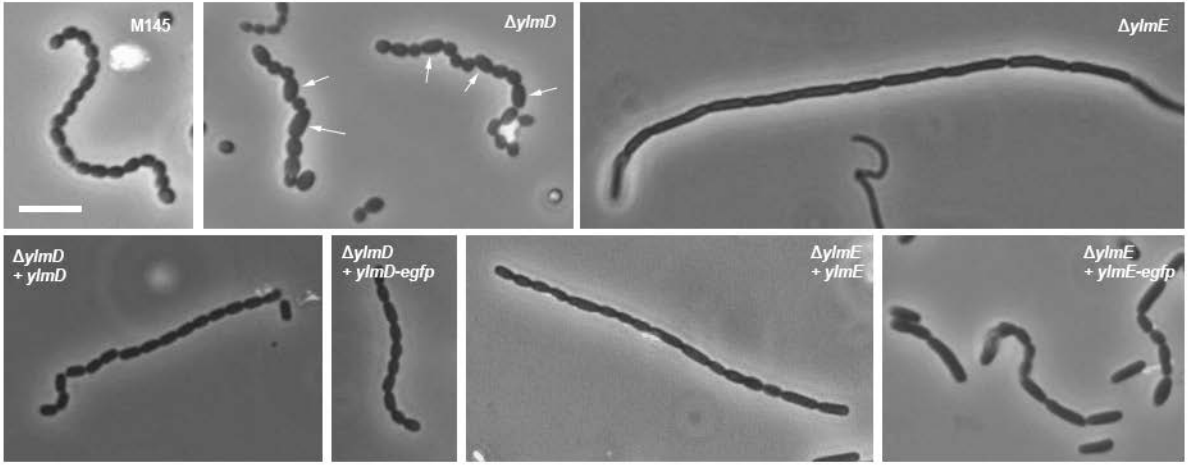
M145
ΔylmD
ΔylmE
ΔylmD
+ ylmD
ΔylmD
+ ylmD-egfp
ΔylmE
+ ylmE
ΔylmE
+ ylmE-egfp

Figure 3

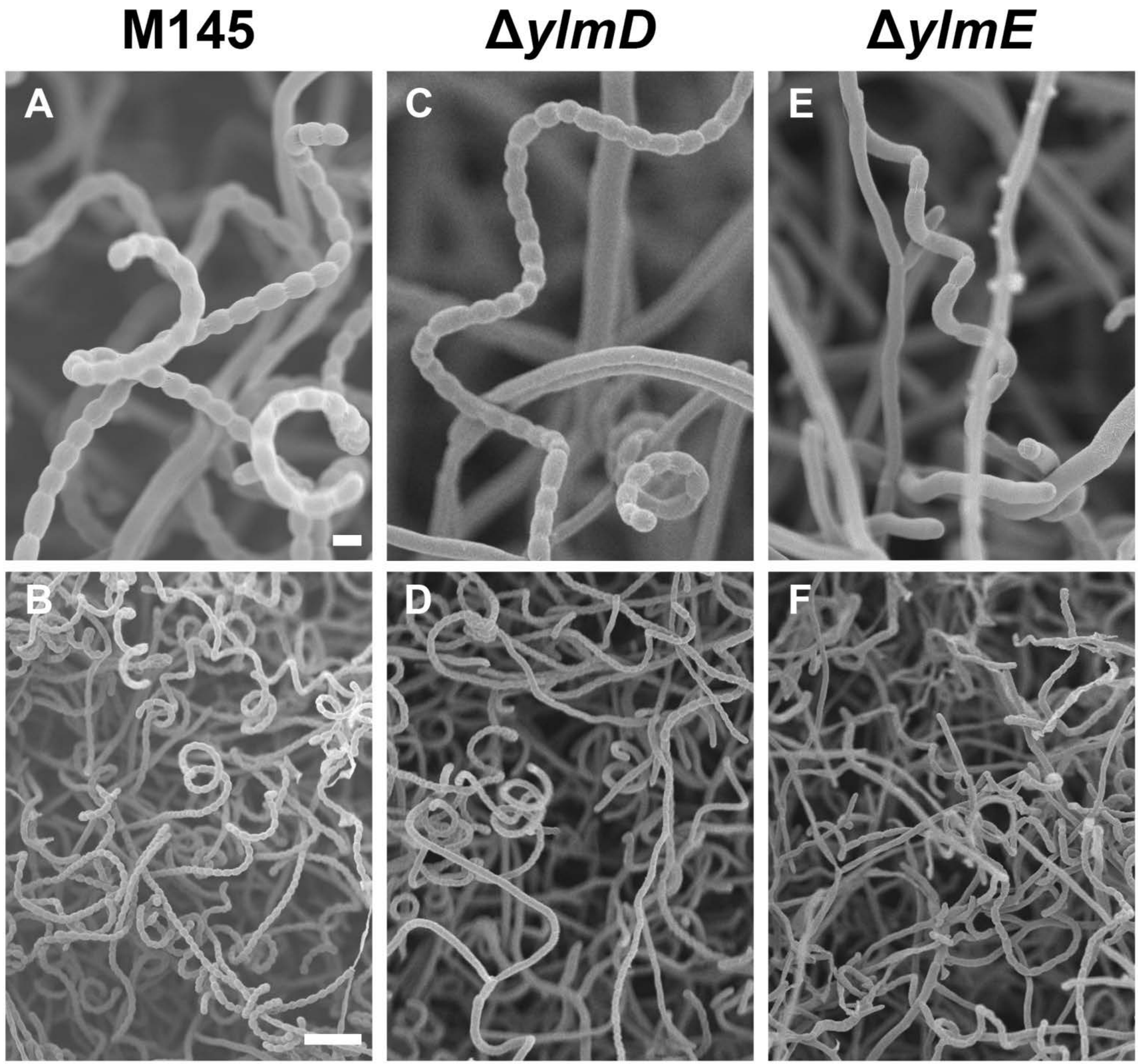

Figure 4

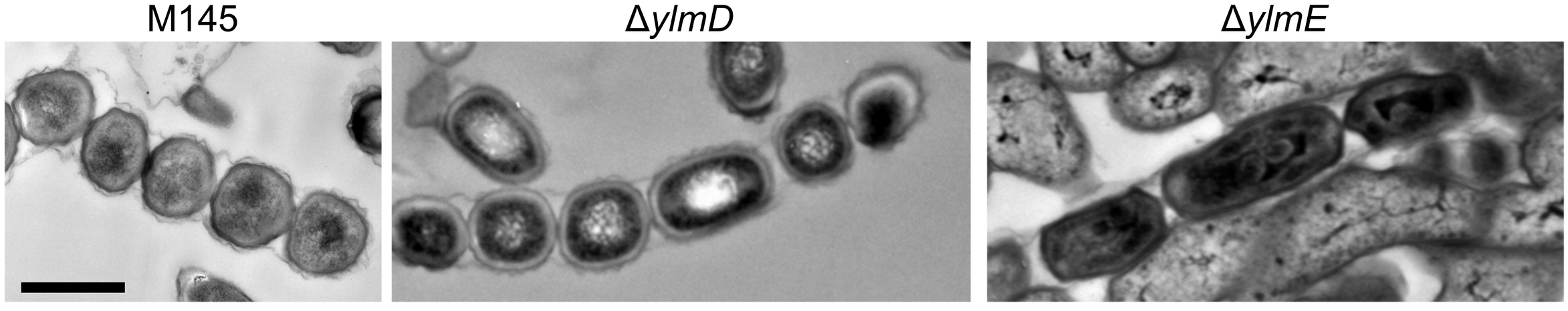

Figure 5A

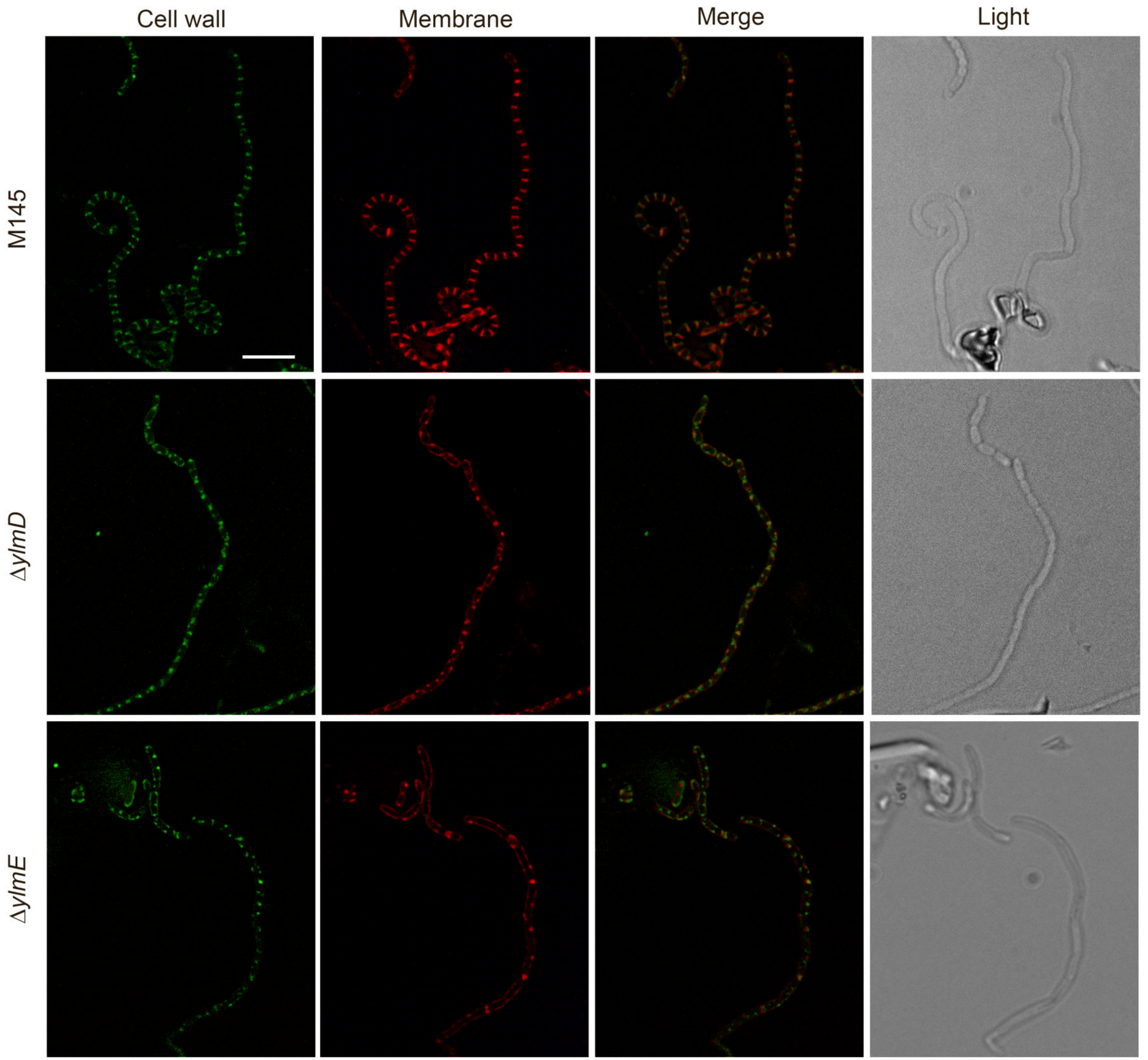

Figure 5B

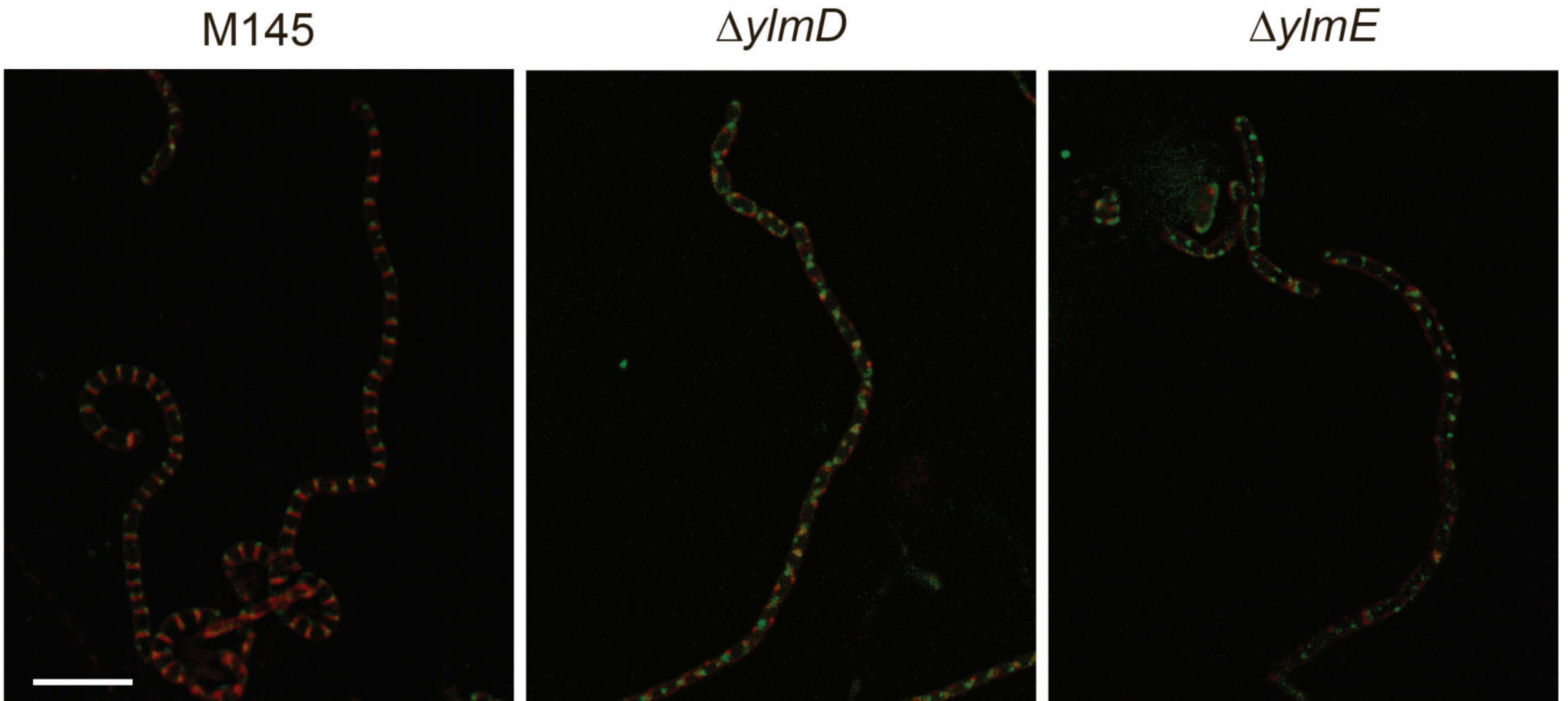

Figure 5C

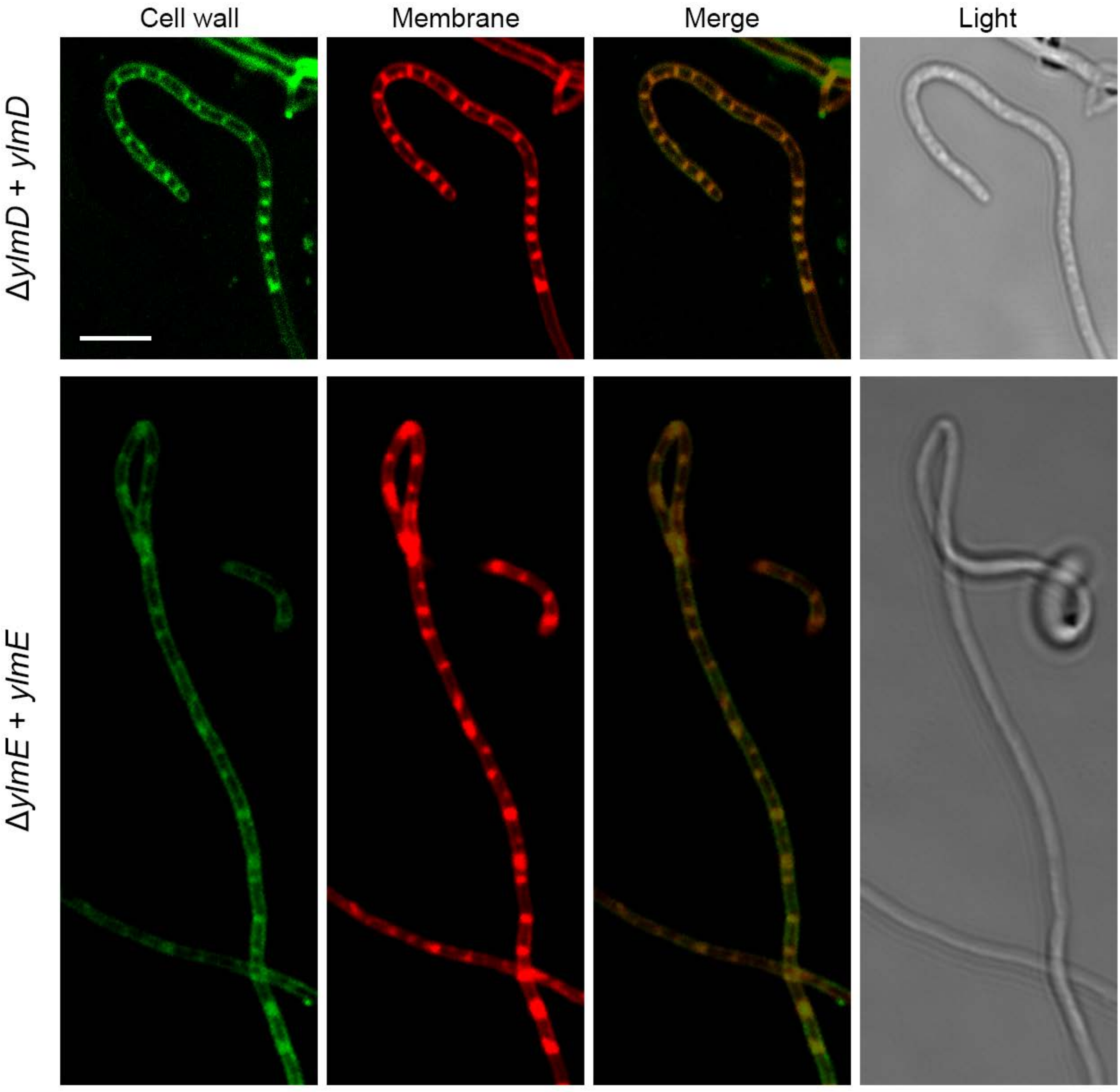

Figure 6

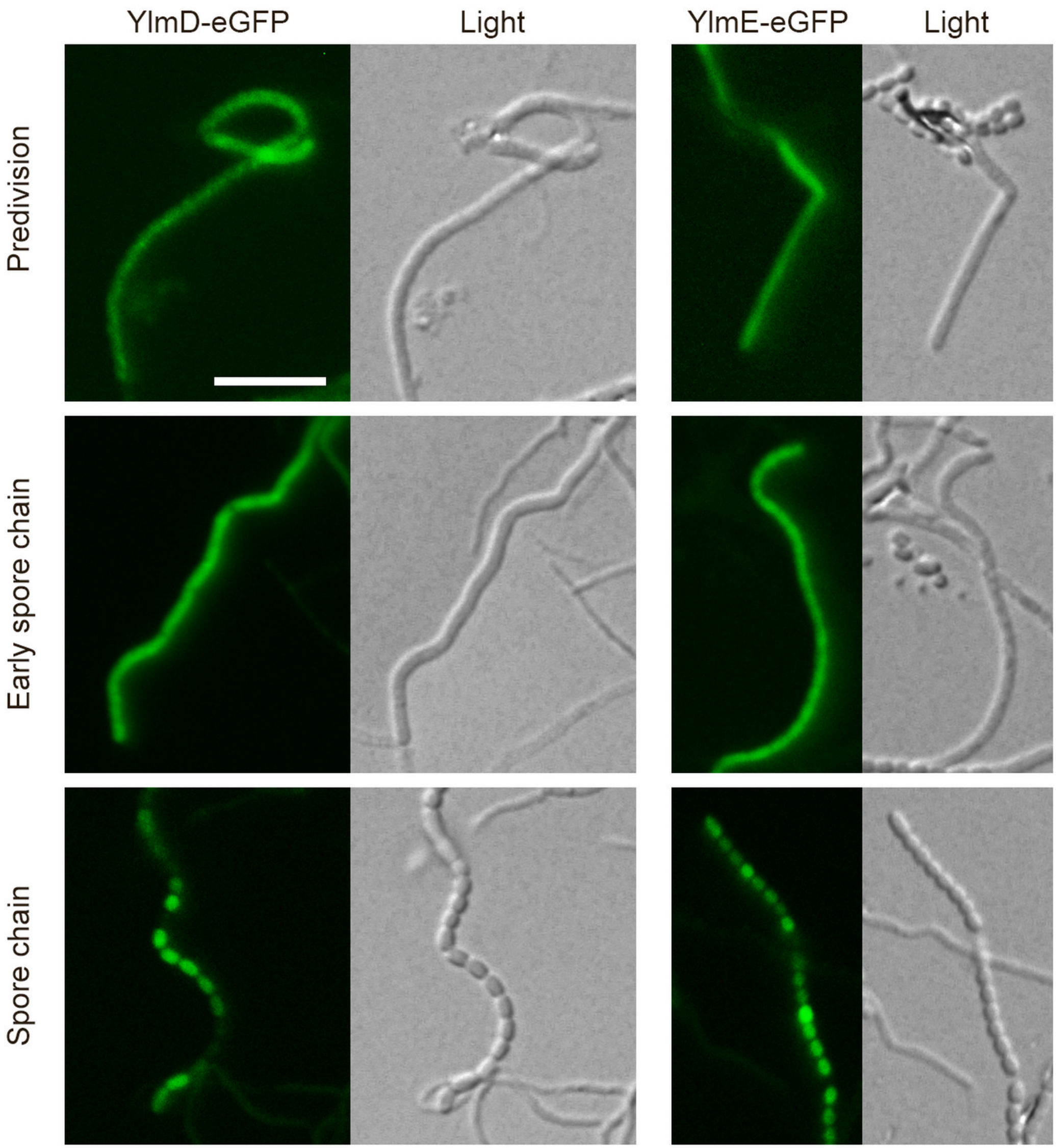
YlmD-eGFP
Light
YlmE-eGFP
Light
Predivision
Early spore chain
Spore chain
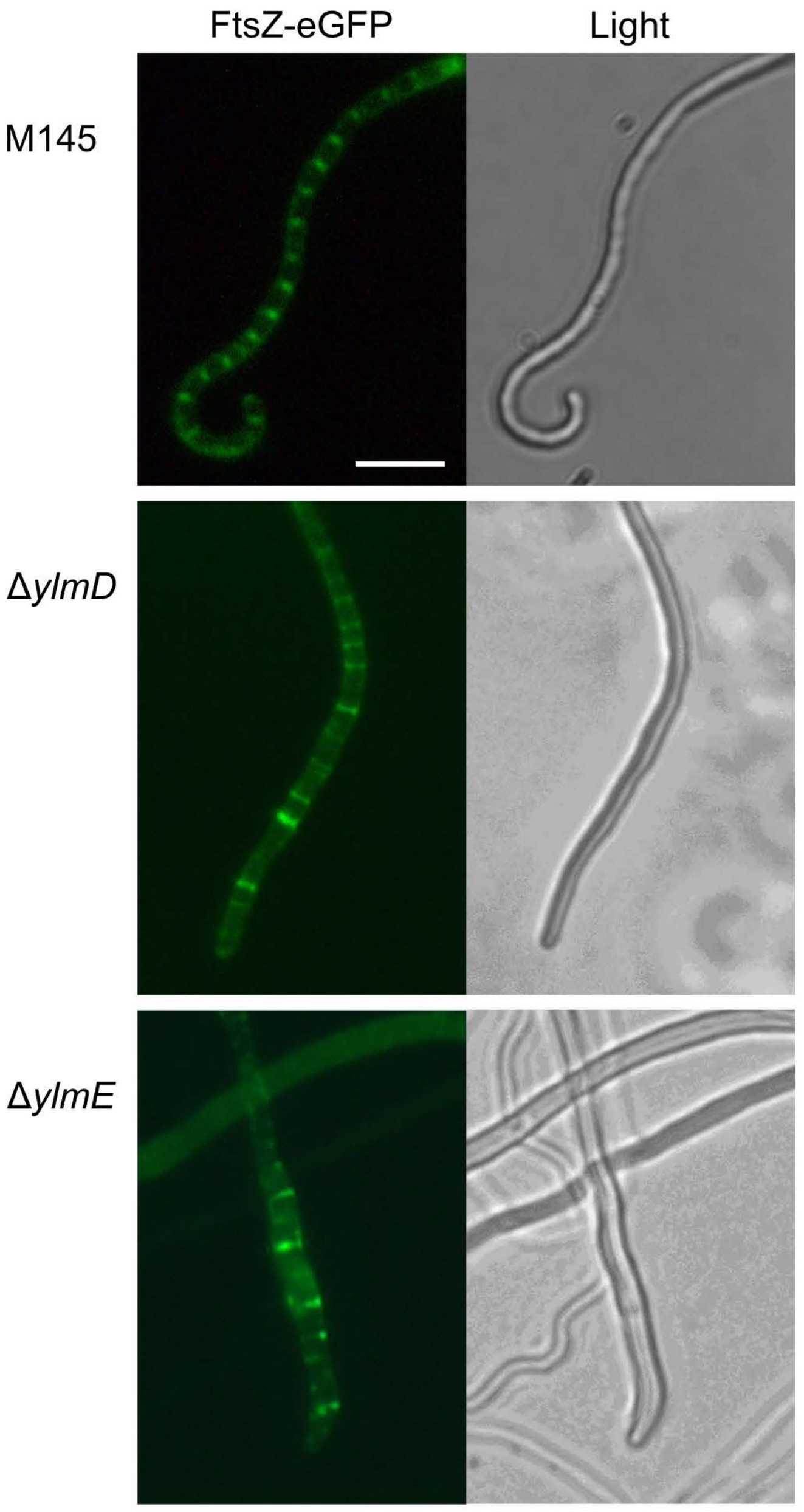
Figure 7